Toxoplasma gondii disrupts β1 integrin signaling and focal adhesion formation during monocyte hypermotility

Received for publication, May 2, 2017, and in revised form, December 14, 2017 Published, Papers in Press, January 2, 2018, DOI 10.1074/jbc.M117.793281

Joshua H. Cook[1], **Norikiyo Ueno**[1], **and Melissa B. Lodoen**[2]

From the Department of Molecular Biology and Biochemistry and the Institute for Immunology, University of California, Irvine, California, 92697

Edited by Velia M. Fowler

The motility of blood monocytes is orchestrated by the activity of cell-surface integrins, which translate extracellular signals into cytoskeletal changes to mediate adhesion and migration. *Toxoplasma gondii* is an intracellular parasite that infects migratory cells and enhances their motility, but the mechanisms underlying *T. gondii*–induced hypermotility are incompletely understood. We investigated the molecular basis for the hypermotility of primary human peripheral blood monocytes and THP-1 cells infected with *T. gondii*. Compared with uninfected monocytes, *T. gondii* infection of monocytes reduced cell spreading and the number of activated β1 integrin clusters in contact with fibronectin during settling, an effect not observed in monocytes treated with lipopolysaccharide (LPS) or *Escherichia coli*. Furthermore, *T. gondii* infection disrupted the phosphorylation of focal adhesion kinase (FAK) at tyrosine 397 (Tyr-397) and Tyr-925 and of the related protein proline-rich tyrosine kinase (Pyk2) at Tyr-402. The localization of paxillin, FAK, and vinculin to focal adhesions and the colocalization of these proteins with activated β1 integrins were also impaired in *T. gondii*–infected monocytes. Using time-lapse confocal microscopy of THP-1 cells expressing enhanced GFP (eGFP)–FAK during settling on fibronectin, we found that *T. gondii*–induced monocyte hypermotility was characterized by a reduced number of enhanced GFP-FAK–containing clusters over time compared with uninfected cells. This study demonstrates an integrin conformation–independent regulation of the β1 integrin adhesion pathway, providing further insight into the molecular mechanism of *T. gondii*–induced monocyte hypermotility.

Monocytes are migratory cells that circulate in the blood and home to sites of infection or injury by extravasating from the bloodstream into tissue (1). This process involves monocyte traversal of the vascular endothelium and the underlying basement membrane and extracellular matrix (ECM)[3]. Cell adhesion and migration are mediated by the activity of cell surface adhesion molecules called integrins, which link extracellular signals to intracellular changes in the actin cytoskeleton (2).

Integrin signaling is initiated by the binding of integrins to ECM or cellular ligands and results in the coordinated formation and disassembly of focal adhesions, the connections that anchor a cell to its substrate. Integrins are noncovalently associated α/β heterodimeric glycoproteins, and each subunit is usually composed of a short, intracellular tail domain, a membrane-spanning helix, and a large ectodomain (3). Inactive integrins are expressed on the cell surface in a low-affinity, bent structure, but can undergo conformational changes to expose the extracellular ligand-binding site upon activation based on talin interactions within the tail domain of the β subunit of the integrin (4, 5). Monocytes regulate this inside-out signaling through the activity of chemokine-activated G protein–coupled receptors (6). Ligand binding to the activated integrins induces receptor clustering and triggers an intracellular signaling cascade. During β1 integrin interactions with fibronectin, integrin clustering recruits structural and signaling proteins to form the focal adhesion complex, which connects integrins to the actin cytoskeleton, thereby establishing a focal adhesion (7).

One component of the focal adhesome is the ubiquitously expressed cytoplasmic tyrosine kinase focal adhesion kinase (FAK) (8–10). As demonstrated by its many roles in embryonic development, cancer progression, and anti-apoptotic pathways (11–12), FAK is a critical signaling protein, consisting of three major domains: a FERM (4.1, ezrin, radixin, moesin) domain, kinase domain, and focal adhesion targeting (FAT) domain. FAK is also a structural protein composed of two proline-rich regions, and it can bind to nascent adhesome components, such as talin (13) and paxillin (14), as well as actin restructuring proteins, such as Arp2/3 (15) and RACK1 (16). In response to β1 integrin clustering, FAK is autophosphorylated at tyrosine residue 397 (p-FAK Tyr-397) to initiate binding with Src via its SH2 and SH3 domains (17). The formation of the FAK-Src complex results in additional phosphorylation of both proteins, leading to maximal downstream effects on actin cytoskeleton

This work was supported by National Institutes of Health Grant R01 AI120846-02 (to M. B. L.), American Cancer Society Grant 126688-RSG-14-202-01-MPC (to M. B. L.), American Heart Association Postdoctoral Fellowships 13POST14580034 and 15POST25550021 (to N. U.), and UCI Undergraduate Research Opportunity Program Grants (to J. H. C.). This work was also supported by the National Center for Research Resources and the National Center for Advancing Translational Sciences, National Institutes of Health, through Grant UL1 TR001414.The authors declare that they have no conflicts of interest with the contents of this article. The content is solely the responsibility of the authors and does not necessarily represent the official views of the National Institutes of Health.

This article contains Figs. S1 and S2, Table S1, and Videos S1 and S2.

[1] These authors contributed equally to this work.

[2] To whom correspondence should be addressed: 3238 McGaugh Hall, Irvine, CA 92617. Tel.: 949-824-7805; Fax: 949-824-8551; E-mail: mlodoen@uci.edu.

[3] The abbreviations used are: ECM, extracellular matrix; FAK, focal adhesion kinase; SH, Src homology; Pyk2, proline-rich tyrosine kinase; DCs, dendritic cells; PE, phycoerythrin.

remodeling (18). FAK null cells are characterized by a defect in focal adhesion disassembly and motility (19).

Monocytes also express a related tyrosine kinase called proline-rich tyrosine kinase (Pyk2, also known as CADTK, RAFTK, CAKβ), which is 45% identical and 66% similar to FAK (20). The two proteins have a similar domain structure and the same relative positioning of their phosphorylation sites (21). Interestingly, alternative splicing of Pyk2 in monocytes results in an isoform that lacks 42 amino acids between the proline-rich regions of the C terminus, resulting in a protein that is 5 kDa smaller (20). The monocyte isoform of Pyk2 localizes to lamellipodia, and disrupting its activity reduces monocyte cell spreading and motility (22). Notably, targeting Pyk2 to focal contacts can rescue the motility of cells deficient in FAK (23).

Toxoplasma gondii is an obligate intracellular parasite capable of infecting and replicating within nucleated cells of warm-blooded animals, and infection of humans can cause severe tissue damage in organs such as the brain and eye (24). Monocytes are recruited to sites of *T. gondii* infection where they can phagocytose and degrade the parasite or become infected themselves (25). One proposed mechanism for *T. gondii* dissemination within an infected host is through parasite invasion of migratory leukocytes, such as monocytes or dendritic cells (DCs). In this model, an infected cell can act as a Trojan horse for *T. gondii* in the bloodstream or tissues (26). Several studies have demonstrated that *T. gondii* infection of monocytes (27, 28), neutrophils (29), natural killer (NK) cells (30), and DCs (31–34) induces a hypermotility phenotype in these cells.

We have previously reported that *T. gondii*–infected monocytes exhibit an impairment of integrin clustering, and in conditions of shear stress, infected cells roll and crawl on vascular endothelium at higher velocities and over greater distances than uninfected monocytes (27, 28). In the current study, we have investigated the downstream consequences of reduced β1 integrin clustering on the activation of FAK and Pyk2 and in focal adhesion formation in *T. gondii*–infected monocytes. We found that infected monocytes formed fewer paxillin-, FAK-, and vinculin-containing focal adhesions and had reduced phosphorylation of FAK Tyr-397 and Tyr-925 and Pyk2 Tyr-402 than did uninfected monocytes during adhesion to fibronectin. Additionally, enhanced GFP (eGFP)–FAK– expressing monocytes infected with *T. gondii* exhibited decreased colocalization of eGFP-FAK and β1 integrins compared with uninfected cells. Furthermore, real-time imaging of human monocytes during cell settling revealed increased motility and fewer eGFP-FAK clusters in infected cells compared with uninfected cells. These findings indicate that the hypermotility of *T. gondii*–infected monocytes is associated with an impairment in the extent of focal adhesion formation downstream of β1 integrin signaling.

Results

Clustering of activated β1 integrins is reduced in T. gondii–infected monocytes settled on fibronectin

The conformational activation of integrins allows for high-affinity interactions with extracellular ligand to mediate cell crawling and arrest (35). We investigated the effect of *T. gondii* infection on the ability of activated β1 integrins to cluster, the initial step in focal adhesion formation. THP-1 monocytic cells were mock infected with media alone or infected with GFP-expressing Type II *T. gondii* for 4 h and settled on fibronectin for 30 min. The cells were imaged at the plane of contact with the fibronectin after staining with a monoclonal antibody that specifically recognizes the activated conformation of β1 integrins (36). Mock-infected cells formed clusters of activated β1 integrins, resembling focal adhesion structures, and spread over the surface of the fibronectin (Fig. 1*A*). Strikingly, there was a dramatic reduction in the clustering of activated β1 integrins in *T. gondii*–infected cells (Fig. 1, *A* and *C*). An analysis of total α4β1 integrin (VLA-4) or activated β1 integrin on the surface of monocytes by flow cytometry (Fig. 1*E*) revealed no differences in infected or uninfected cells, indicating that *T. gondii* caused a reduction in activated integrin clustering to ligand without affecting integrin cell surface expression.

To determine whether the disruption in β1 integrin clustering was specific to *T. gondii* infection or simply because of monocyte activation, we also examined β1 integrin clustering in THP-1 cells treated with lipopolysaccharide or exposed to *Escherichia coli* and settled onto fibronectin (Fig. 1*B*). In the *T. gondii* and *E. coli* conditions, the cells were imaged both at the cell base and in the z-plane at the cell center to permit visualization of the intracellular pathogen. In contrast to *T. gondii* infection, neither LPS nor *E. coli* impaired β1 integrin clustering, as cells in these conditions exhibited similar or higher numbers of β1 integrin clusters compared with mock-treated cells (Fig. 1*C*). Although differences in the surface area of β1 integrin clusters in each condition did meet statistical detection (Fig. 1*D*), the magnitude of these changes was small, suggesting that *T. gondii* infection predominantly affected the number of β1 integrin clusters in adherent cells, rather than the size of the clusters. The *T. gondii*-induced impairment in activated β1 integrin clustering was also observed when we examined total α4β1 integrin (Fig. S1). Taken together, these data indicate that *T. gondii* dysregulation of β1 integrin clustering in infected monocytes is not a general feature of microbial stimulation.

Focal adhesion signaling is disrupted downstream of β1 integrins

To investigate the downstream effects of a decrease in β1 integrin clustering on the adhesome complex, we examined a key regulator of integrin signaling and focal adhesion formation, focal adhesion kinase. Freshly elutriated human peripheral blood monocytes were mock infected or infected with *T. gondii* for 4 h and either left unsettled or settled on fibronectin. Lysates from the cells were prepared after 15, 30, or 60 min post settling or from control unsettled cells, and Western blotting was performed for total FAK and p-FAK Tyr-397, the initial autophosphorylation event induced by β1 integrin clustering (Fig. 2*A*). In mock-treated cells settled on fibronectin, an increase in p-FAK Tyr-397 was observed as early as 15 min after settling and persisted at 30 min. In contrast, there was no comparable induction in the levels of p-FAK Tyr-397 in cells infected with *T. gondii* (Fig. 2*B*).

In addition to FAK, monocytes highly express the related kinase proline-rich tyrosine kinase 2 (Pyk2). By qPCR analysis,

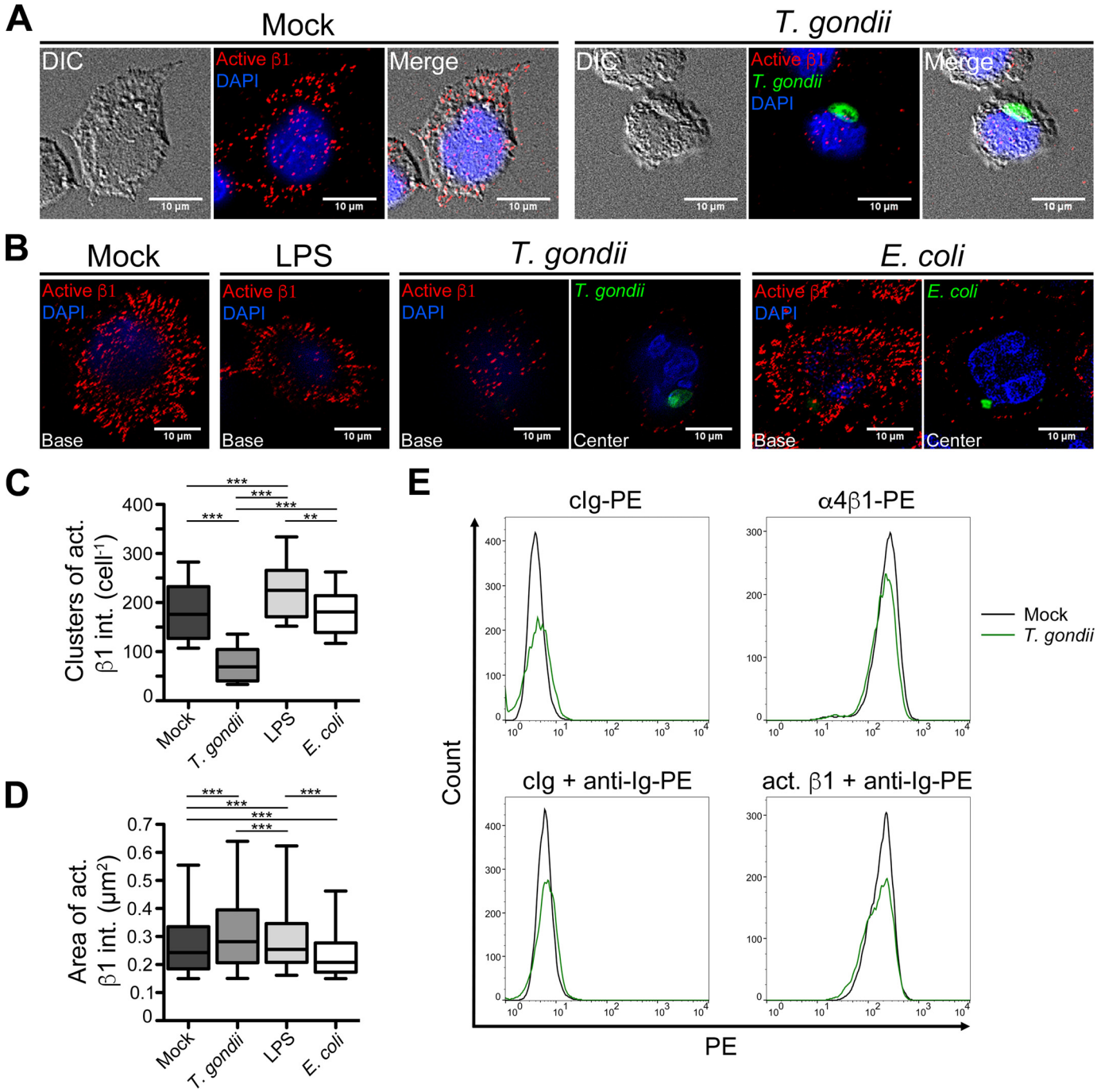

Figure 1. Activated β1 integrin clustering in human monocytic cells. *A*, THP-1 cells were mock infected or infected with GFP-expressing *T. gondii* for 4 h, settled onto fibronectin-coated coverslips for 30 min, fixed, and stained with a mAb specific for the active (open and extended) conformation of β1 integrins and DAPI. Micrographs of mock-infected cells and cells harboring *T. gondii* were acquired at the cell base in contact with fibronectin. Representative images from five independent experiments are shown. *B*, THP-1 monocytic cells were mock treated or cultured with LPS, GFP-expressing *T. gondii* or CFSE-labeled *E. coli* for 4 h and settled onto fibronectin-coated coverslips. The cells were fixed and stained for the active conformation of β1 integrins and DAPI. Micrographs were acquired at the cell base and at the cell center in the *T. gondii* and *E. coli* conditions to permit visualization of the intracellular microbes (in *green*). Representative images from four independent experiments are shown. *C* and *D*, for all conditions in (*B*), the number (*C*) and area (*D*) of activated β1 integrin clusters per cell were calculated using the method published by Horzum *et al.* (58). $n = 2000$ randomly selected β1 integrin clusters from 50–84 cells in each condition. In all the box-and-whisker plots, the whiskers represent the 5th and 95th percentiles (*i.e.* not the standard deviation). **, $p < 0.01$; ***, $p < 0.001$; one-way ANOVA with a Bonferroni post hoc test. *E*, THP-1 cells were mock infected (*black histograms*) or infected with *T. gondii* (*green histograms*) for 4 h, stained with a control Ig (*clg*), anti-α4β1 (VLA-4) integrin mAb, or anti-activated β1 integrin mAb, and analyzed by flow cytometry. Representative histograms from three independent experiments are shown.

transcripts for both *PTK2* and *PTK2B* (the gene names of FAK and Pyk2, respectively) were detected in freshly elutriated monocytes (Fig. 2*D*). *PTK2B* transcripts were more abundantly expressed than *PTK2* relative to *GAPDH*, consistent with previous reports that monocytes predominately express Pyk2 (20). Given the potential role for Pyk2 in focal adhesion formation in monocytes, we also investigated total Pyk2 and the phosphorylation of tyrosine residue 402 (p-Pyk2 Tyr-402) in infected pri-

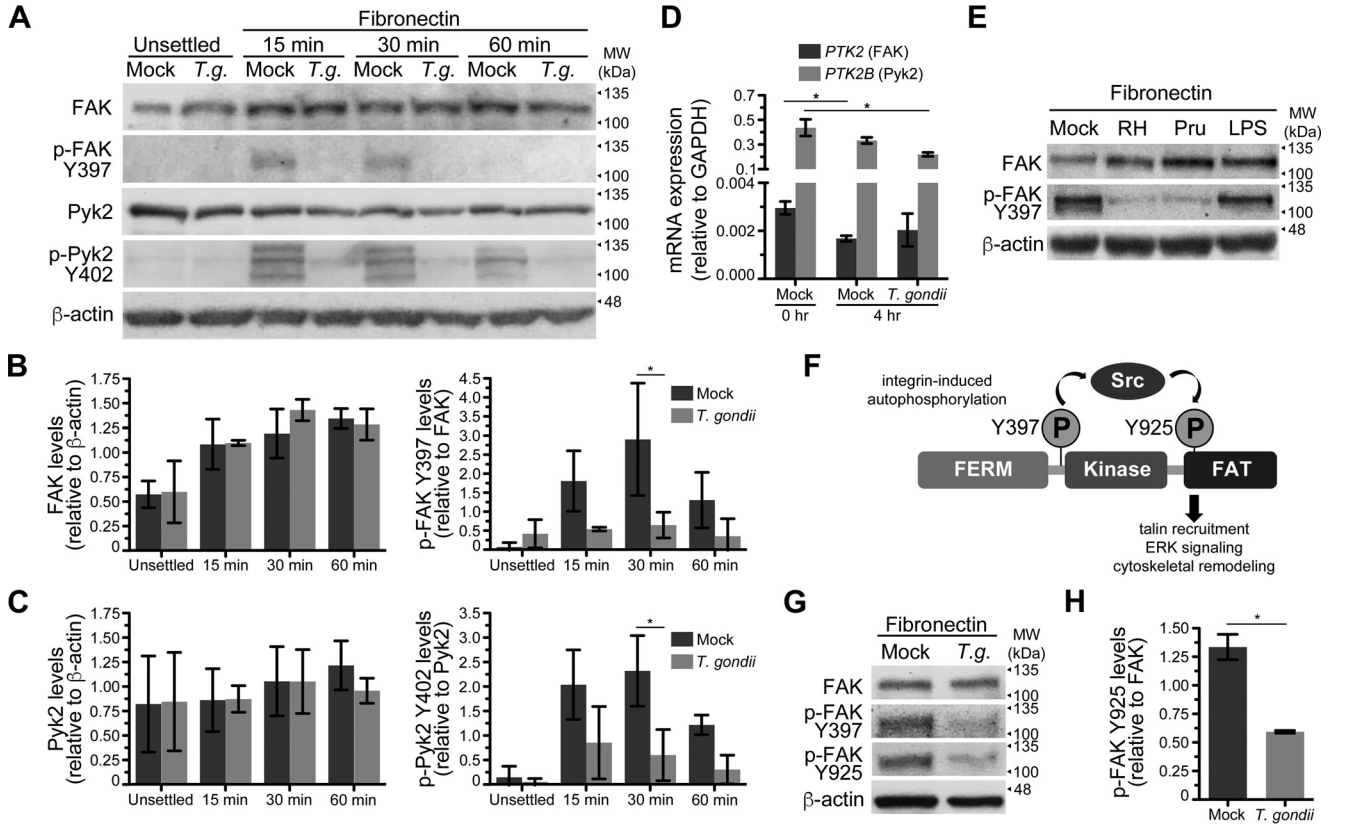

Figure 2. Phosphorylation of FAK and Pyk2 in monocytes during cell adhesion. *A*, primary human monocytes were mock infected or infected with *T. gondii* for 4 h and either lysed in suspension or settled on fibronectin for 15, 30, or 60 min prior to lysis. Total lysates were separated by SDS-PAGE and examined by Western blotting for total FAK, p-FAK Tyr-397, total Pyk2, p-Pyk2 Tyr-402, and β-actin. Molecular weight markers (*MW*) are shown to the right of each blot. Representative blots from three independent experiments are shown. *B* and *C*, densitometry was performed on Western blots of FAK (*B*) and Pyk2 (*C*) by normalizing band intensities to β-actin. p-FAK Tyr-397 and p-Pyk2 Tyr-402 levels were normalized to total FAK or total Pyk2 band intensities, respectively. *Error bars* display the mean ± S.D. from three independent experiments (*, $p < 0.05$; one-way ANOVA with a Bonferroni post hoc test). *D*, transcript levels of *PTK2* and *PTK2B* (the gene names for FAK and Pyk2, respectively) relative to *GAPDH* were quantified by qPCR. RNA was isolated from freshly elutriated primary human monocytes (0 h) or monocytes cultured for 4 h in mock conditions or with *T. gondii*. *Error bars* indicate the mean ± S.D. from three independent experiments. (*, $p < 0.05$; **, $p < 0.01$; one-way ANOVA with a Bonferroni post hoc test). *E*, primary human monocytes were mock treated or cultured with *T. gondii* of Type I (RH strain) or Type II (*Prugniaud* strain) lineage for 4 h or treated with LPS. Monocytes were then settled onto immobilized fibronectin, lysed, and analyzed by Western blotting using antibodies for total FAK, p-FAK Tyr-397, and β-actin. Representative blots from three independent experiments are shown. *F*, a simplified model of FAK phosphorylation and subsequent FAK-mediated signaling for cell adhesion is illustrated. Autophosphorylation at Tyr-397 induces FAK association with Src and signals for adhesome formation. The association results in Src phosphorylation of FAK at Tyr-925, located within the C-terminal focal adhesion targeting (*FAT*) domain. *G*, primary human monocytes were mock infected or cultured with *T. gondii* for 4 h, settled onto fibronectin for 30 min, lysed, and analyzed by Western blotting using antibodies for total FAK, p-FAK Tyr-397, p-FAK Tyr-925, and β-actin. Representative blots from four independent experiments are shown. *H*, quantification of p-FAK Tyr-925 levels relative to total FAK at 30 min post settling was performed by using densitometry of Western blots. *Error bars* display the mean ± S.D. from four independent experiments. (*, $p < 0.05$; Student's *t*-test).

mary monocytes settled on fibronectin, in parallel with tracking total FAK and p-FAK Tyr-397 (Fig. 2, *A* and *C*). Tyr-402 of Pyk2 is functionally analogous to Tyr-397 of FAK (37). Notably, the reduced detection of p-Pyk Tyr-402 recapitulated the reduced levels of p-FAK Tyr-397 in *T. gondii*–infected cells. Interestingly, in two out of three blood donors, we detected three bands with the antibody against p-Pyk2 Tyr-402, which may reflect detection of the previously reported splice variants of Pyk2 (20).

Infection of monocytes with either Type I (RH) or Type II (*Prugniaud*) *T. gondii* resulted in reduced levels of p-FAK Tyr-397, but this effect was not observed in monocytes treated with LPS (Fig. 2*E*), indicating a specific effect of *T. gondii* infection.

The formation of focal adhesion structures and signaling for actin cytoskeletal rearrangements involves interactions between Src kinase and FAK, culminating in the Src-dependent phosphorylation of Tyr-925 of FAK (38) (Fig. 2*F*). *T. gondii* infection also resulted in a significant reduction in the phosphorylation of Tyr-925 of FAK (Fig. 2, *G* and *H*), suggesting a defect in the formation of the FAK-Src complex in infected cells. Collectively, these data on the phosphorylation of Pyk2 and FAK demonstrate a disruption of focal adhesion signaling in *T. gondii*-infected monocytes downstream of β1 integrin activation.

FAK, paxillin, and vinculin localization to focal adhesions is impaired in T. gondii–infected monocytes

During the formation of nascent focal adhesions, FAK is recruited to the cytoplasmic tails of β1 integrins (39). To study the dynamics of FAK localization during the adhesion of *T. gondii*–infected cells, we used retroviral transduction to generate a line of THP-1 monocytic cells expressing an eGFP-FAK fusion protein (called eGFP-FAK THP-1 cells) (Fig. 3*A*). Among the transduced cells, there was heterogeneity in eGFP-FAK expression. Single-cell clones were isolated using limiting dilution to create a homogeneous population of eGFP-FAK expressing cells (Fig. 3*B*). Lysates from uninfected or *T. gondii*–infected

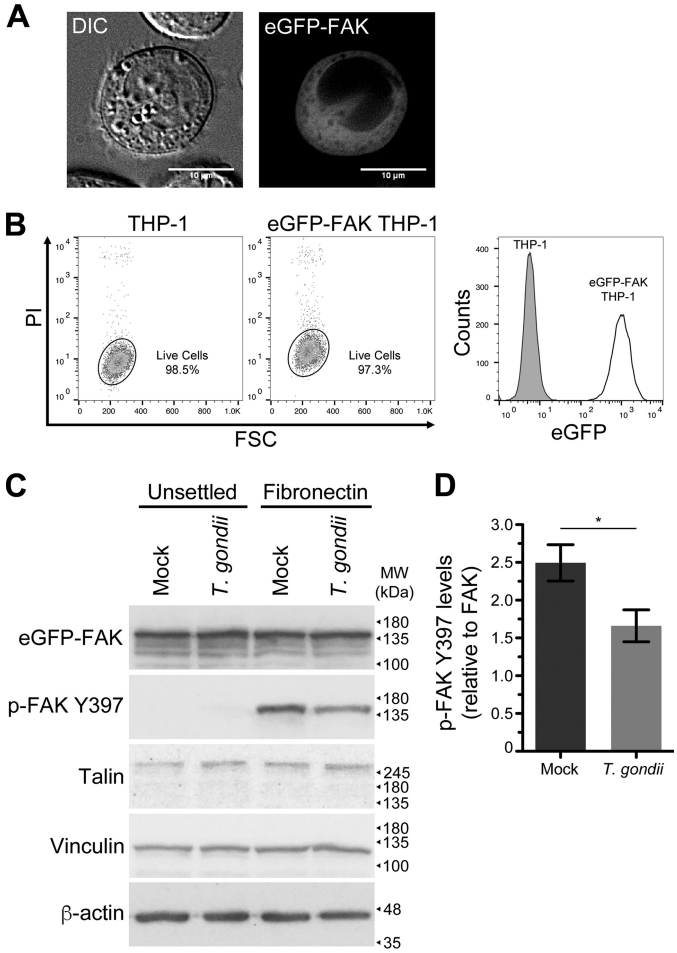

Figure 3. Generation of eGFP-FAK THP-1 cells. *A*, eGFP-FAK was expressed in THP-1 monocytic cells by retroviral transduction, and the cells were imaged by live cell fluorescence microscopy. *B*, the transduced cells were single-cell cloned, and the clonal population was compared with the parental THP-1 cells by flow cytometry. Debris and dead cells were gated out based on a propidium iodide (PI) viability stain, and eGFP expression of the THP-1 and eGFP-FAK THP-1 cells was represented as histograms. *C*, eGFP-FAK THP-1 cells were mock infected or infected with *T. gondii* for 4 h and left unsettled or settled onto fibronectin for 30 min. Cells were lysed and analyzed by Western blotting using antibodies for total eGFP-FAK, phosphorylated eGFP-FAK at Tyr-397 (p-FAK Tyr-397), talin, vinculin, and β-actin. Representative blots from four independent experiments are shown. *D*, densitometry was performed on Western blots of p-FAK Tyr-397 by normalizing band intensities to total FAK. *Error bars* display the mean ± S.D. from four independent experiments (*, $p < 0.05$; Student's *t*-test).

eGFP-FAK THP-1 cells that were unsettled or settled on fibronectin were probed by Western blotting for eGFP-FAK and for phosphorylated eGFP-FAK at Tyr-397 (hereafter referred to as p-FAK Tyr-397 in these cells), along with additional components of the adhesome (Fig. 3*C*). Although less dramatic than in cells expressing only endogenous FAK, *T. gondii* infection of the eGFP-FAK cells also resulted in lower levels of p-FAK Tyr-397 compared with mock infection (Fig. 3, *C* and *D*). The reduced magnitude of the effect of infection on p-FAK Tyr-397 in the eGFP-FAK THP-1 cells may indicate that the parasite is less effective at inhibiting the phosphorylation of FAK when FAK is highly overexpressed, as in the eGFP-FAK cells (Fig. S2). The levels of the adhesome components talin and vinculin were unchanged in the mock and *T. gondii*–infected eGFP-FAK THP-1 cells (Fig. 3*C*).

Utilizing the eGFP-FAK THP-1 cells, we examined the recruitment of FAK to clusters of activated β1 integrins. The cells were mock infected or infected with Type II tdTomato-expressing *T. gondii* for 4 h, and settled on fibronectin for 15, 30, or 60 min. The cells were then fixed and stained for activated β1 integrins (Fig. 4*A*). The z-plane at the center of infected cells was also imaged to permit visualization of the intracellular parasites in the cytosol, as indicated by the *arrows*. The surface area of the infected cells was significantly reduced compared with uninfected cells at each time point examined, indicating a reduction in cell spreading over fibronectin because of infection (Fig. 4*B* and Table S1). By quantifying the area and number of eGFP-FAK adhesions per cell, we observed a significant decrease in the number of adhesions per cell in infected compared with the uninfected cells, suggesting that infection reduced the density of adhesions (Fig. 4*C*). Furthermore, the colocalization of eGFP-FAK and activated β1 integrins in infected and uninfected cells was calculated using Manders' coefficient, in which a value closer to 1 indicates a greater degree of spatial overlap in signals (40). A reduced colocalization of eGFP-FAK and activated β1 integrins was observed in the *T. gondii*-infected cells compared with uninfected cells (Fig. 4*C* and Table S1). Finally, we also examined the localization of the focal adhesion components paxillin and vinculin, indicators of nascent and mature focal adhesions, respectively, in mock and *T. gondii*–infected THP-1 cells during settling (Fig. 5, *A* and *B*) and found that infection resulted in a significant reduction in the number of adhesions marked by either paxillin or vinculin and in the colocalization of both of these proteins with β1 integrin (Fig. 5*C* and Table S1). There was also a statistically detectable reduction in the area of adhesions marked by either paxillin or vinculin (Fig. 5*C*), although the magnitude of these changes was not large. Collectively, these data suggest that the decrease in p-FAK Tyr-397 and p-Pyk2 Tyr-402 in infected cells resulted from fewer β1 integrin clusters and was associated with an impairment of paxillin, FAK, and vinculin localization to focal adhesions.

Live microscopy confirms impaired focal adhesion formation in T. gondii–infected cells

To observe the organization of FAK during focal adhesion formation, the clonal line of eGFP-FAK THP-1 cells (Fig. 3*B*) was live imaged by time-lapse confocal microscopy during a settling period of 40 min on fibronectin (Fig. 6*A* and Videos S1 and S2). Uninfected monocytes spread over the fibronectin surface and formed structures resembling focal adhesions, which were visible as small regions of high eGFP-FAK density (Fig. 6*A*). Notably, these structures increased in mock-infected cells over time, particularly during the first 15 min of settling, after which point, they appeared to stabilize (Fig. 6*B*). In contrast, *T. gondii*–infected cells formed fewer aggregations of eGFP-FAK, with no net increase over time (Fig. 6*B*). Most notably, the *T. gondii*–infected cells changed shape rapidly as they roamed over the ECM (Fig. 6, *A* and *C* and Video S2) and moved at significantly higher speeds (Fig. 6*D*) than uninfected cells, consistent with the increased motility of *T. gondii*–infected monocytes (28) and the microscopy analyses of cells fixed at specific time points after settling on fibronectin (Fig. 4*A*).

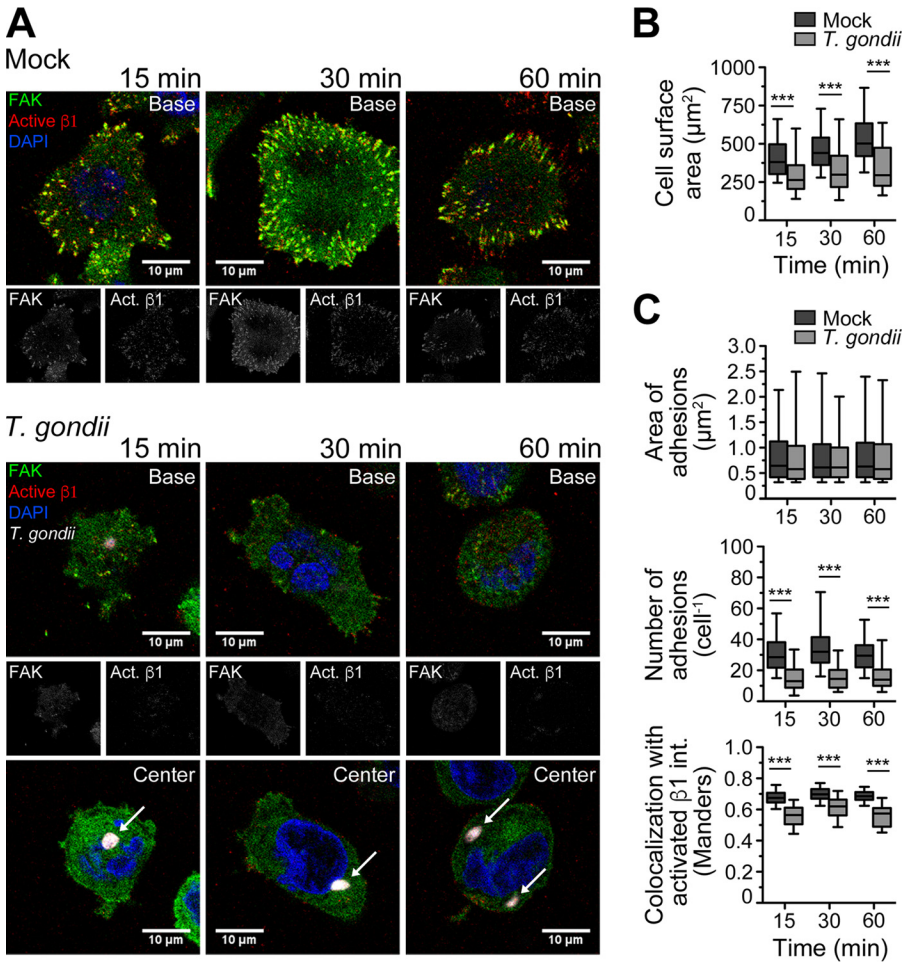

Figure 4. Localization of eGFP-FAK and activated β1 integrins during cell adhesion. eGFP-FAK THP-1 cells were mock infected or infected with *T. gondii* for 4 h and settled onto fibronectin-coated coverslips. *A*, at the designated times, cells were fixed and stained with DAPI and for β1 integrins using an active conformation-specific mAb. Confocal micrographs of mock-infected and *T. gondii*–infected cells were acquired at the cell base, and micrographs of cells harboring *T. gondii* were acquired at the cell base and cell center to visualize intracellular parasites (*arrows*). Representative images from three independent experiments are shown. *B*, the surface area of the cell base of mock and infected monocytes was quantified. *C*, the area and number of adhesions containing eGFP-FAK per cell were measured using previously described methods (58). The colocalization of eGFP-FAK with activated β1 integrin at the cell base was measured using Manders' coefficient. *B* and *C*, $n = 600$ randomly selected β1 integrin clusters from 61–112 cells in each condition. (***, $p < 0.001$; one-way ANOVA with a Bonferroni post hoc test).

Discussion

Integrins function as critical regulators of cell adhesion and motility in immune cells and are characterized by bidirectional signaling. They assume an open, extended "activated" conformation through inside-out signaling, and also transduce signals from extracellular ligands to intracellular pathways via outside-in signaling. Several studies have demonstrated that immune cells infected with *T. gondii* become hypermotile (27–34, 41), an effect that has been proposed to facilitate the dissemination of the intracellular parasite in the infected host. In the present study, we have demonstrated that the hypermotility of *T. gondii*–infected human monocytes is linked to a dysregulation in integrin-dependent cell adhesion through defects in FAK-regulated focal adhesions. Notably, *T. gondii* infection did not affect the expression of integrins on the cell surface (Fig. 1*E*) or the ability of integrins to become activated through inside-out signaling (27). Rather, *T. gondii* impeded outside-in signaling and integrin clustering upon ligand engagement. These findings are consistent with the hypothesis that the level of activated integrins expressed on the cell surface does not necessarily predict the adhesive properties of the cell (42). Interestingly, although integrin clustering is impaired in *T. gondii*–infected monocytes, these cells, nonetheless, require functional integrins for crawling on cellular substrates, as blocking integrins or their ligands with neutralizing antibodies prevents *T. gondii*–induced hypermotility (28). Taken together, these findings indicate that the parasite modulates the activity of integrins on infected monocytes, rather than blocking integrin function completely.

The *T. gondii*–induced disruption in integrin-mediated adhesion is linked to a dysregulation of components of the focal adhesion complex. In response to extracellular ligand binding, focal adhesion proteins are recruited to the complex in a hierarchical manner. FAK is a key regulator of the assembly and disassembly of focal adhesions and functions as both a signaling kinase and a scaffolding protein in the focal adhesome. In the autoinhibited state, the FERM domain of FAK structurally inhibits the kinase domain, and it is the displacement of the FERM domain that allows for the initiation of the kinase activity of FAK and autophosphorylation of Tyr-397 (43). FAK then

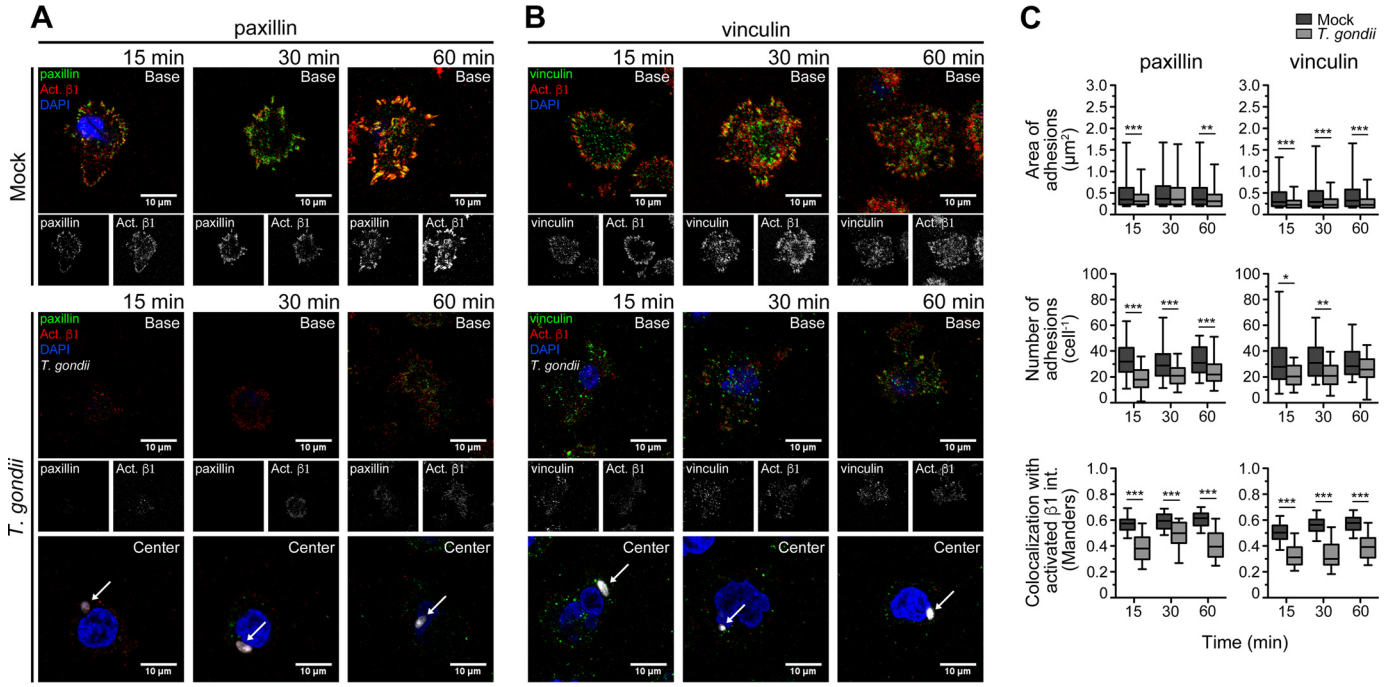

Figure 5. Localization of paxillin and vinculin to activated β1 integrins during cell adhesion. THP-1 cells were mock infected or infected with *T. gondii* for 4 h and settled onto fibronectin-coated coverslips. *A* and *B*, at the designated times, cells were fixed and stained with DAPI and with antibodies for activated β1 integrin and either paxillin (*A*) or vinculin (*B*). The cells were imaged by confocal microscopy at the plane of contact with fibronectin to permit visualization of the adhesions, and the infected cells were also imaged at the middle of the cell to capture the intracellular parasites (*arrows*). Representative images from four independent experiments are shown. *C*, the area and number of adhesions containing paxillin or vinculin per cell were measured using previously described methods (58). The colocalization of paxillin and vinculin with activated β1 integrin at the cell base was measured using Manders' coefficient. $n = 600$ randomly selected β1 integrin clusters from 55–84 cells in each condition (*, $p < 0.05$; **, $p < 0.01$; ***, $p < 0.001$; one-way ANOVA with a Bonferroni post hoc test).

recruits talin (13), which may function as the architectural framework for the adhesome machinery (44, 45). The knockout of FAK in mice results in embryonic lethality because of a defect in mesoderm development, and interestingly, cells from these embryos have reduced motility, indicating a role for FAK in focal adhesion disassembly (19). In FAK-null cells, key adhesome proteins such as paxillin, talin, and vinculin localize to the cell periphery more slowly, resulting in a delay in actin restructuring. In addition, focal adhesion turnover is severely reduced (46). Based on the reduced mobility of FAK knock-out mouse embryonic fibroblasts, it is perhaps surprising that *T. gondii*–induced hypermotility in monocytes is associated with a reduction in FAK phosphorylation. However, it has also been shown that FAK knockdown leads to increased motility of cancer cells and fibroblasts (47), suggesting that FAK regulation of motility may also be dependent on the expression and function of other components of the focal adhesome. Indeed, Pyk2 expression increases in FAK knock-out mouse embryonic fibroblasts (48), endothelial cells (49), and mammary tumor cells (50), and Pyk2 can functionally substitute for FAK in these cells, supporting a compensatory function of Pyk2 in the motility of FAK-deficient cells. In our studies, we have observed a reduction in 1) p-FAK Tyr-397 and p-Pyk2 Tyr-402; 2) FAK, paxillin, and vinculin recruitment to focal adhesions; and 3) the total number of focal adhesions formed in *T. gondii*–infected monocytes during settling. Although additional mechanisms aside from FAK and Pyk2 activation may contribute to parasite-induced hypermotility, our data suggest that *T. gondii* impairs focal adhesion formation. We, therefore, favor the hypothesis that the parasite-induced dysregulation occurs after integrin binding/activation and before FAK phosphorylation in the signaling pathway connecting fibronectin to the actin cytoskeleton.

The conformational activation of integrins has been heavily studied, as it is a primary mechanism of regulating integrin function. However, the regulation of outside-in signaling through integrin clustering remains less well understood. Kindlins, although structurally similar to talin, occupy nonredundant roles in integrin-mediated signaling and recycling, and bind to β integrins at a separate NP*X*Y motif (42). Kindlin-2, although not required for α5β1-mediated adhesion of endothelial cells (42), facilitates integrin αIIbβ3 clustering in Chinese hamster ovary cells during binding to fibrinogen (51). Additionally, the interactions between kindlin-2 and integrin-linked kinase (ILK) are necessary for outside-in αIIbβ3 integrin signaling and cell adhesion, although mutations preventing this binding do not affect integrin activation (52). It is possible that *T. gondii* disrupts kindlin function in infected monocytes, dysregulating β1 integrin outside-in signaling, but not inside-out signaling. As a result, monocyte-sustained adhesion is reduced, yet the cells maintain the ability to migrate and cross endothelial barriers. Of course, further studies examining the localization, activation, and binding interactions of kindlins are necessary to elucidate their role in *T. gondii* infection–induced hypermotility.

T. gondii is known to manipulate host cells via proteins secreted into the cell during invasion or released when the parasite is harbored within the specialized parasitophorous vacuole (53). Recently, it was found that *T. gondii* secretes a 14-3-3 protein (Tg14-3-3) into the parasitophorous vacuole and sequesters host 14-3-3 (54), a family of adapter proteins

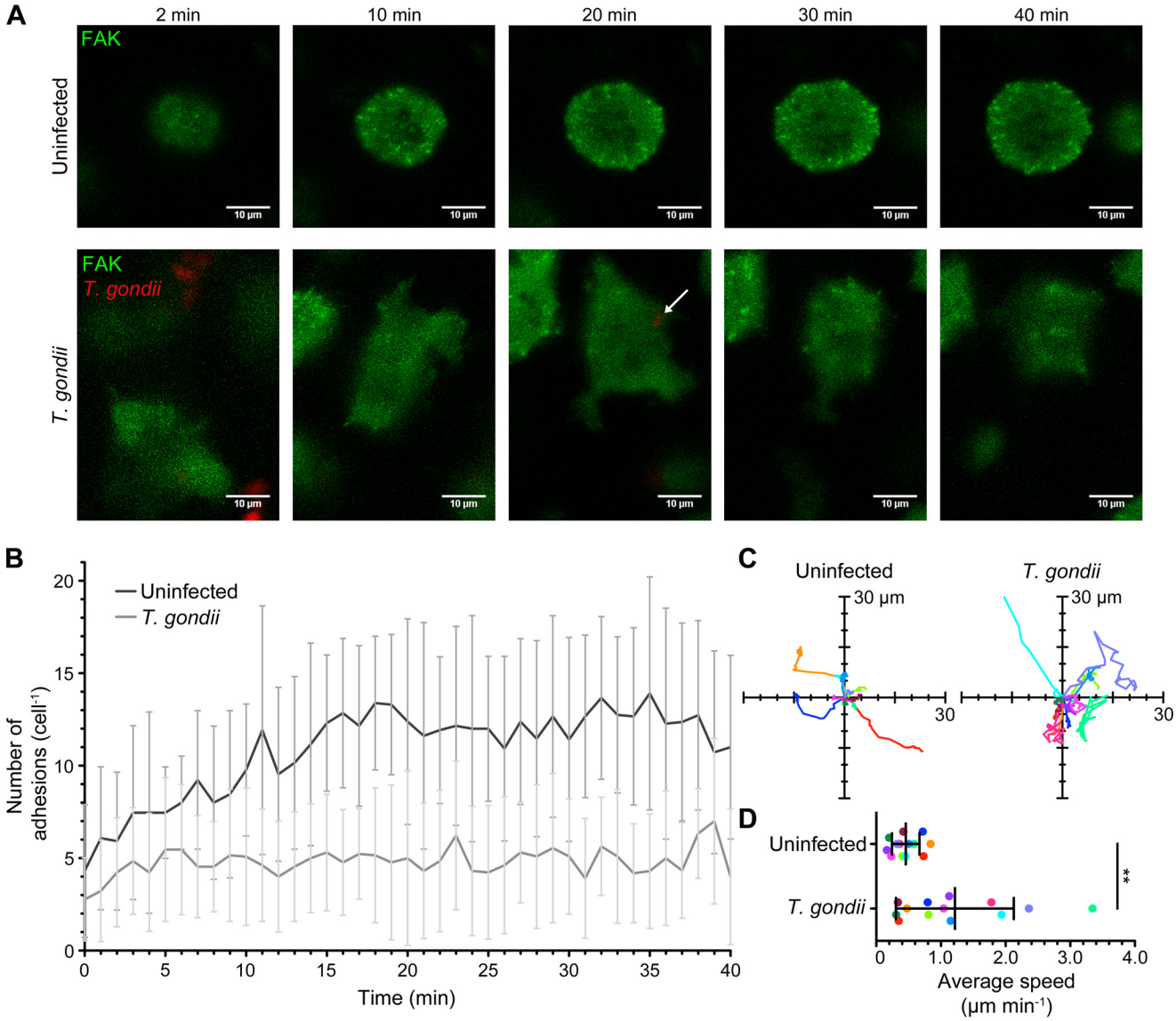

Figure 6. Real-time microscopy of FAK recruitment to the contact interface during cell adhesion and motility. Uninfected or *T. gondii*–infected eGFP-FAK THP-1 cells were settled onto fibronectin-coated chamber slides and imaged on a confocal microscope in an environmental chamber maintained at 37 °C and 5% CO_2. The cells were imaged as z-stacks for 40 min at a frequency of 1 stack per min. *A*, images shown are five sequential frames summed together (t-projection) with the time stamp indicating the time point of the middle frame. The *arrow* indicates an intracellular *T. gondii*. These filmstrips are representative of videos from 14 independent experiments. *B*, the number of adhesions formed by uninfected or *T. gondii*–infected eGFP-FAK THP-1 cells was measured over time using previously established methods (58). $n = 13$ cells in each condition ($p < 0.001$ for infection and $p = 0.7950$ for time, using a two-way ANOVA). *C*, flower plots depict the path lengths of individual uninfected or *T. gondii*–infected eGFP-FAK THP-1 cells during imaging. Each track represents the path of a single cell rooted at the origin. *D*, the average speed of the cells tracked in (*B*) and (*C*) during imaging is shown. Each dot represents a single cell, and the colors of the dots correspond with the colors of the tracks in (*B*) (**, $p < 0.01$; Student's *t*-test).

involved in numerous signaling pathways including adhesion. The introduction of purified Tg14-3-3 into DCs or the expression of Tg14-3-3 in DCs is sufficient to induce hypermotility (54). In addition, a peptide from the *T. gondii* dense granule protein GRA5 increases the CCR7-mediated chemotaxis of DCs (55). There is also evidence that soluble *T. gondii* proteins can affect immune cell chemotaxis, as cyclophilin-18 (C-18), a soluble protein secreted by *T. gondii*, recruits DCs (56) in a CCR5-dependent manner.

The current report demonstrates a disruption to FAK and Pyk2 activation in *T. gondii*–infected monocytes, which may underlie monocyte hypermotility. These findings provide another example of *T. gondii* manipulation of cellular adhesion, interestingly, by impairing integrin-mediated clustering without affecting integrin expression or conformational activation. Because FAK, through its various binding partners and protein substrates, lies at the junction of many intracellular signaling pathways, these findings also suggest that *T. gondii* dysregulation of FAK activation may have broader implications for parasite manipulation of host cell signaling platforms.

Experimental procedures

Mammalian and parasite cell culture and infections

THP-1 monocytic cells were grown in RPMI 1640 medium (GE Healthcare) supplemented with 10% heat-inactivated fetal

bovine serum (FBS) (Omega Scientific, Tarzana, CA), 2 mM L-glutamine, 100 units ml^{-1} penicillin, and 100 $\mu g\ ml^{-1}$ streptomycin (R-10%). Primary monocytes were isolated from peripheral blood mononuclear cells (PBMC) using counterflow elutriation, as described previously (28). Isolated primary monocytes were resuspended in R-10% and used immediately. Blood was collected by the University of California, Irvine Institute for Clinical and Translational Science in accordance with guidelines and approval of the University of California, Irvine Institutional Review Board.

Type II *Prugniaud* parasites expressing tdTomato or GFP and Type I RH parasites expressing GFP were grown in human foreskin fibroblasts (HFFs) maintained in Dulbecco's modified Eagle medium (DMEM) (GE Healthcare) with 10% heat-inactivated FBS, 2 mM L-glutamine, 100 units ml^{-1} penicillin, and 100 $\mu g\ ml^{-1}$ streptomycin (D-10%), as previously described (57). For infection experiments of THP-1 or primary monocytes, infected human foreskin fibroblasts were syringe lysed and washed once with D-10%. The lysate was filtered through a 5-μm low protein binding Durapore® membrane (EMD Millipore), washed with D-10%, and resuspended in R-10%. Parasites were added to the monocytes at a multiplicity of infection (m.o.i.) of 2 to 3 and incubated at 37 °C for 3 to 4 h before the cells were used in settling assays. Mock-infected cells are those in which the same volume of R-10% media that was used for the parasite infections was added to the monocytes in place of parasites. All parasite and mammalian cell cultures were tested monthly for *Mycoplasma* contamination and confirmed to be negative.

Retroviral transduction

eGFP-FAK–expressing THP-1 cells were generated using retroviral transduction. The pMXs-puro-eGFP-FAK plasmid, deposited by Noboru Mizushima (University of Tokyo, Japan), was purchased from Addgene (Cambridge, MA). 293T Phoenix A cells were transfected with the plasmid using Lipofectamine LTX (Thermo Fisher Scientific) to produce replication-incompetent retrovirus. THP-1 cells were infected with retrovirus by centrifugation at 2500 rpm for 3 h at 25 °C. Three days post transduction, the cells were selected in R-10% with 2 $\mu g\ ml^{-1}$ puromycin. Single-cell cloning by serial dilution produced a line of THP-1 with uniform levels of eGFP-FAK expression. eGFP-FAK expression of clonal isolates was confirmed by flow cytometry using a BD FACSCalibur analyzer (BD Biosciences), and the data were analyzed by FlowJo software (FlowJo, Ashland, OR).

E. coli and LPS treatment

E. coli were resuspended in the cytoplasmic dye carboxyfluorescein succinimidyl ester (CFSE) (Thermo Fisher Scientific) and washed with PBS before addition to THP-1 cells. Where indicated, THP-1 cells were treated with 100 $\mu g\ ml^{-1}$ of LPS in R-10%.

Immunofluorescence microscopy and adhesion analysis

To investigate cell settling, 3×10^5 uninfected or *T. gondii*–infected monocytes were settled onto fibronectin-coated glass coverslips for 15, 30, or 60 min at 37 °C. The samples were fixed with 4% paraformaldehyde (Electron Microscopy Sciences, Hatfield, PA), blocked with PBS and 5% normal goat serum (SouthernBiotech, Birmingham, AL), permeabilized with 0.01% saponin (Sigma-Aldrich), and probed with antibodies against activated β1 integrins (12G10, EMD Millipore) (36), VLA-4 (9F10, BioLegend, San Diego, CA), paxillin (mAb ab32084, Abcam, Cambridge, MA), or vinculin (pAb ab73412, Abcam). Alexa Fluor 488 conjugated goat anti-rabbit IgG, Alexa Fluor 594 conjugated goat anti-mouse IgG, or Alexa Fluor 647 conjugated goat anti-mouse IgG (Thermo Fisher Scientific) were used as secondary antibodies. The coverslips were mounted to slides using VectaShield with DAPI (Vector Laboratories, Burlingame, CA).

The cells were imaged using either a Nikon Eclipse Ti inverted microscope with a CFI Plan Apo VC 60× oil immersion objective with a 1.4 numerical aperture (Nikon Instruments Inc., Melville, NY) or a Leica TCS SP8 confocal microscope with a HC PL Apochromat 63× oil immersion objective with a 1.4 numerical aperture (Leica Microsystems GmbH, Menarini, Germany). Surface area and Manders' coefficient were computed by a self-designed MATLAB (The MathWorks, Inc., Natick, MA) program: github.com/LodoenLab/FAK-Paper.[4] The Manders' coefficient was determined using the algorithm described by Manders *et al.* (40). The identification and measurement of adhesions in microscopy images was conducted using ImageJ (National Institutes of Health, Bethesda, MD) following the algorithm published by Horzum *et al.* (58). The algorithm was modified to optimize adhesion identification in our microscopy images: the Laplacian of Gaussian filter was not used, the rolling ball radius for background subtraction was set at 10 pixels, and the minimum size for particle detection was set at 0.15 μm. The algorithm can be found here: github.com/LodoenLab/FAK-Paper.[4] Graphs were generated using Prism (GraphPad Software, Inc., La Jolla, CA).

Flow cytometry

Mock and *T. gondii*–infected THP-1 cells were resuspended in fluorescence-activated cell sorting (FACS) buffer (PBS with 2% FBS) containing the Fc receptor blocking solution, Human TruStain FcX (BioLegend, San Diego, CA). The cells were incubated on ice for 10 min then resuspended in a control IgG-phycoerythrin (PE) (MOPC-21, BioLegend), anti-α4β1 integrin-PE antibody (9F10, BioLegend), unconjugated control IgG (MOPC-21), or anti-activated β1 integrin antibody (12G10, EMD Millipore). The cells were incubated for 30 min on ice, and excess antibody was removed by washing with FACS buffer. The cells stained with the unconjugated control IgG or the anti-activated β1 integrin antibodies were incubated with PE goat anti-mouse IgG antibodies for 15 min on ice. The cells were acquired by flow cytometry (BD FACSCalibur, BD Biosciences), and the data were analyzed using FlowJo software (FlowJo).

[4] Please note that the JBC is not responsible for the long-term archiving and maintainance of this site or any other third party hosted site.

Statistics

One-way or two-way analysis of variance (ANOVA) or Student's *t*-test were used for statistical analysis, as indicated in the figure legends. For the one-way ANOVA, a Bonferroni post hoc test was used. For all the box-and-whisker plots, the boxes represent the first and third quartiles, the band represents the median, and the whiskers represent the 5th and 95th percentiles.

Western blotting and densitometry

Cell lysates were prepared with 2× Laemmli buffer and 10% β-mercaptoethanol, and 2×10^5 cell equivalents for each sample were loaded and separated on 10% SDS-PAGE. Gels were transferred to polyvinylidene difluoride (PVDF) (Bio-Rad, Hercules, CA) and probed using antibodies for FAK (D2R2E), phospho-FAK Tyr-397 (D20B1), or polyclonal antibodies against phospho-FAK Tyr-925, Pyk2 (H364), phospho-Pyk2 Tyr-402 from Cell Signaling Technology (Danvers, MA); vinculin (7F9) or talin (TA205) from EMD Millipore; or β-actin (AC-15, Sigma Aldrich). The membranes were then probed with HRP-conjugated anti-mouse or anti-rabbit IgG (Jackson ImmunoResearch, West Grove, PA) and visualized using enhanced chemiluminescence (GE Healthcare Life Sciences). Images were captured by a Nikon camera as described previously (27). Band intensity was quantified using ImageJ Gel tools (National Institutes of Health, Bethesda, MD).

Time-lapse videomicroscopy

Live imaging was performed on a Zeiss Laser Scanning Microscope 780 (Zeiss, Oberkochen, Germany) using an incubation chamber maintained at 37 °C and 5% CO_2. Eight-chambered Lab-Tek no. 1.0 borosilicate cover glasses (Thermo Fisher Scientific) were coated with fibronectin for 1 h prior to use. Images were captured as z-stacks 0.5 μm apart starting from just below the cell base to the top of the cell at a frequency of 1 min^{-1}.

qPCR

RNA was extracted using the RNeasy Mini Kit (Qiagen, Germantown, MD) and treated with DNase I (Thermo Fisher Scientific). cDNA was synthesized using SuperScript III First-Strand Synthesis kit (Thermo Fisher Scientific). Relative gene expression was quantified using iQ SYBR Green Supermix (Bio-Rad, Hercules, CA), an iCycler PCR system (Bio-Rad), and the cycle threshold (Ct) method (59), where the levels of expression have been normalized to levels of the housekeeping gene *GAPDH*. The primers used for *GAPDH* have been previously described (60). The *PTK2* and *PTK2B* (the gene names of FAK and Pyk2, respectively) primers were as follows: *PTK2*, 5′-GCTGCAATCCCACACATCTT-3′ (sense) and 5′-TCCGCAATGGTTAGGGATGG-3′ (antisense); *PTK2B*, 5′-TGTGAAGCTGGGGGACTTTG-3′ (sense) and 5′-AGGATCTCCCACATGCACAC-3′ (antisense). All primers were designed such that the amplicon spanned an intron/exon boundary. All PCR was performed in triplicate and with the following negative controls: samples without SuperScript III reverse transcriptase or with water in the place of a DNA template, and no signal was observed in these samples.

Author contributions—M. B. L. conceived and coordinated the research and supervised the project. N. U. and J. H. C. designed, performed, and analyzed the experiments. J. H. C. and M. B. L. wrote the manuscript. All authors reviewed the results and approved the final version of the manuscript.

Acknowledgments—We thank all members of the Lodoen, Morrissette, and Tenner labs for helpful discussion on this project. We especially thank Dr. Naomi Morrissette, Dr. Michelle Digman, and Dr. Enrico Gratton for suggestions and advice. We also thank Dr. Adeela Syed for training and assistance at the UCI Optical Biology Core Facility and the staff of the UC Irvine Institute for Clinical and Translational Science for coordinating healthy volunteers for blood donation.

References

1. Imhof, B. A., and Aurrand-Lions, M. (2004) Adhesion mechanisms regulating the migration of monocytes. *Nat. Rev. Immunol.* **4,** 432–444 CrossRef Medline
2. Ley, K., Laudanna, C., Cybulsky, M. I., and Nourshargh, S. (2007) Getting to the site of inflammation: The leukocyte adhesion cascade updated. *Nat. Rev. Immunol.* **7,** 678–689 CrossRef Medline
3. Ginsberg, M. H., Partridge, A., and Shattil, S. J. (2005) Integrin regulation. *Curr. Opin. Cell Biol.* **17,** 509–516 CrossRef Medline
4. Luo, B.-H., Carman, C. V., and Springer, T. A. (2007) Structural basis of integrin regulation and signaling. *Annu. Rev. Immunol.* **25,** 619–647 CrossRef Medline
5. Shattil, S. J., Kim, C., and Ginsberg, M. H. (2010) The final steps of integrin activation: The end game. *Nat. Rev. Mol. Cell Biol.* **11,** 288–300 CrossRef Medline
6. Laudanna, C., Kim, J. Y., Constantin, G., and Butcher, E. (2002) Rapid leukocyte integrin activation by chemokines. *Immunol. Rev.* **186,** 37–46 CrossRef Medline
7. Mitra, S. K., Hanson, D. A., and Schlaepfer, D. D. (2005) Focal adhesion kinase: In command and control of cell motility. *Nat. Rev. Mol. Cell Biol.* **6,** 56–68 CrossRef Medline
8. Schaller, M. D., Borgman, C. A., Cobb, B. S., Vines, R. R., Reynolds, A. B., and Parsons, J. T. (1992) pp125FAK a structurally distinctive protein-tyrosine kinase associated with focal adhesions. *Proc. Natl. Acad. Sci. U.S.A.* **89,** 5192–5196 CrossRef Medline
9. Hanks, S. K., Calalb, M. B., Harper, M. C., and Patel, S. K. (1992) Focal adhesion protein-tyrosine kinase phosphorylated in response to cell attachment to fibronectin. *Proc. Natl. Acad. Sci. U.S.A.* **89,** 8487–8491 CrossRef Medline
10. Guan, J. L., and Shalloway, D. (1992) Regulation of focal adhesion-associated protein tyrosine kinase by both cellular adhesion and oncogenic transformation. *Nature* **358,** 690–692 CrossRef Medline
11. Schlaepfer, D. D., Mitra, S. K., and Ilic, D. (2004) Control of motile and invasive cell phenotypes by focal adhesion kinase. *Biochim. Biophys. Acta* **1692,** 77–102 CrossRef Medline
12. Sulzmaier, F. J., Jean, C., and Schlaepfer, D. D. (2014) FAK in cancer: mechanistic findings and clinical applications. *Nat. Rev. Cancer.* **14,** 598–610 CrossRef Medline
13. Lawson, C., Lim, S. T., Uryu, S., Chen, X. L., Calderwood, D. A., and Schlaepfer, D. D. (2012) FAK promotes recruitment of talin to nascent adhesions to control cell motility. *J. Cell Biol.* **196,** 223–232 CrossRef Medline
14. Turner, C. E. (2000) Paxillin interactions. *J. Cell Sci.* **113,** 4139–4140 Medline
15. Serrels, B., Serrels, A., Brunton, V. G., Holt, M., McLean, G. W., Gray, C. H., Jones, G. E., and Frame, M. C. (2007) Focal adhesion kinase controls actin assembly via a FERM-mediated interaction with the Arp2/3 complex. *Nat. Cell Biol.* **9,** 1046–1056 CrossRef Medline
16. Serrels, B., Sandilands, E., Serrels, A., Baillie, G., Houslay, M. D., Brunton, V. G., Canel, M., Machesky, L. M., Anderson, K. I., and Frame, M. C. (2010) A

complex between FAK, RACK1, and PDE4D5 controls spreading initiation and cancer cell polarity. *Curr. Biol.* **20,** 1086–1092 CrossRef Medline
17. Thomas, J. W., Ellis, B., Boerner, R. J., Knight, W. B., White, G. C., 2nd, and Schaller, M. D. (1998) SH2- and SH3-mediated interactions between focal adhesion kinase and Src. *J. Biol. Chem.* **273,** 577–583 CrossRef Medline
18. Ruest, P. J., Roy, S., Shi, E., Mernaugh, R. L., and Hanks, S. K. (2000) Phosphospecific antibodies reveal focal adhesion kinase activation loop phosphorylation in nascent and mature focal adhesions and requirement for the autophosphorylation site. *Cell Growth Differ.* **11,** 41–48 Medline
19. Ilić, D., Furuta, Y., Kanazawa, S., Takeda, N., Sobue, K., Nakatsuji, N., Nomura, S., Fujimoto, J., Okada, M., and Yamamoto, T. (1995) Reduced cell motility and enhanced focal adhesion contact formation in cells from FAK-deficient mice. *Nature* **377,** 539–544 CrossRef Medline
20. Li, X., Hunter, D., Morris, J., Haskill, J. S., and Earp, H. S. (1998) A calcium-dependent tyrosine kinase splice variant in human monocytes. Activation by a two-stage process involving adherence and a subsequent intracellular signal. *J. Biol. Chem.* **273,** 9361–9364 CrossRef Medline
21. Lev, S., Moreno, H., Martinez, R., Canoll, P., Peles, E., Musacchio, J. M., Plowman, G. D., Rudy, B., and Schlessinger, J. (1995) Protein tyrosine kinase PYK2 involved in Ca^{2+}-induced regulation of ion channel and MAP kinase functions. *Nature* **376,** 737–745 CrossRef Medline
22. Watson, J. M., Harding, T. W., Golubovskaya, V., Morris, J. S., Hunter, D., Li, X., Haskill, J. S., and Earp, H. S. (2001) Inhibition of the calcium-dependent tyrosine kinase (CADTK) blocks monocyte spreading and motility. *J. Biol. Chem.* **276,** 3536–3542 CrossRef Medline
23. Klingbeil, C. K., Hauck, C. R., Hsia, D. A., Jones, K. C., Reider, S. R., and Schlaepfer, D. D. (2001) Targeting Pyk2 to β1-integrin–containing focal contacts rescues fibronectin-stimulated signaling and haptotactic motility defects of focal adhesion kinase–null cells. *J. Cell Biol.* **152,** 97–110 CrossRef Medline
24. Montoya, J. G., and Remington, J. S. (2008) Clinical practice: Management of *Toxoplasma gondii* infection during pregnancy. *Clin. Infect. Dis.* **47,** 554–566 CrossRef Medline
25. Dunay, I. R., and Sibley, L. D. (2010) Monocytes mediate mucosal immunity to Toxoplasma gondii. *Curr. Opin. Immunol.* **22,** 461–466 CrossRef Medline
26. Courret, N., Darche, S., Sonigo, P., Milon, G., Buzoni-Gâtel, D., and Tardieux, I. (2006) CD11c- and CD11b-expressing mouse leukocytes transport single *Toxoplasma gondii* tachyzoites to the brain. *Blood.* **107,** 309–316 CrossRef Medline
27. Harker, K. S., Ueno, N., Wang, T., Bonhomme, C., Liu, W., and Lodoen, M. B. (2013) *Toxoplasma gondii* modulates the dynamics of human monocyte adhesion to vascular endothelium under fluidic shear stress. *J. Leukoc. Biol.* **93,** 789–800 CrossRef Medline
28. Ueno, N., Harker, K. S., Clarke, E. V., McWhorter, F. Y., Liu, W. F., Tenner, A. J., and Lodoen, M. B. (2014) Real-time imaging of *Toxoplasma*-infected human monocytes under fluidic shear stress reveals rapid translocation of intracellular parasites across endothelial barriers. *Cell Microbiol.* **16,** 580–595 CrossRef Medline
29. Coombes, J. L., Charsar, B. A., Han, S. J., Halkias, J., Chan, S. W., Koshy, A. A., Striepen, B., and Robey, E. A. (2013) Motile invaded neutrophils in the small intestine of *Toxoplasma gondii*-infected mice reveal a potential mechanism for parasite spread. *Proc. Natl. Acad. Sci. U.S.A.* **110,** E1913–E1922 CrossRef Medline
30. Ueno, N., Lodoen, M. B., Hickey, G. L., Robey, E. A., and Coombes, J. L. (2015) *Toxoplasma gondii*–infected natural killer cells display a hypermotility phenotype *in vivo*. *Immunol. Cell Biol.* **93,** 508–513 CrossRef Medline
31. Lambert, H., Hitziger, N., Dellacasa, I., Svensson, M., and Barragan, A. (2006) Induction of dendritic cell migration upon *Toxoplasma gondii* infection potentiates parasite dissemination. *Cell Microbiol.* **8,** 1611–1623 CrossRef Medline
32. Weidner, J. M., Kanatani, S., Hernández-Castañeda, M. A., Fuks, J. M., Rethi, B., Wallin, R. P. A., and Barragan, A. (2013) Rapid cytoskeleton remodelling in dendritic cells following invasion by *Toxoplasma gondii* coincides with the onset of a hypermigratory phenotype. *Cell Microbiol.* **15,** 1735–1752 CrossRef Medline
33. Fuks, J. M., Arrighi, R. B. G., Weidner, J. M., Kumar Mendu, S., Jin, Z., Wallin, R. P. A., Rethi, B., Birnir, B., and Barragan, A. (2012) GABAergic signaling is linked to a hypermigratory phenotype in dendritic cells infected by *Toxoplasma gondii*. *PLoS Pathog.* **8,** e1003051 CrossRef Medline
34. Kanatani, S., Uhlén, P., and Barragan, A. (2015) Infection by *Toxoplasma gondii* induces amoeboid-like migration of dendritic cells in a three-dimensional collagen matrix. *PLoS One* **10,** 1–16 CrossRef Medline
35. Iwamoto, D. V., and Calderwood, D. A. (2015) Regulation of integrin-mediated adhesions. *Curr. Opin. Cell Biol.* **36,** 41–47 CrossRef Medline
36. Su, Y., Xia, W., Li, J., Walz, T., Humphries, M. J., Vestweber, D., Cabañas, C., Lu, C., and Springer, T. A. (2016) Relating conformation to function in integrin α5β1. *Proc. Natl. Acad. Sci. U.S.A.* **113,** E3872–E3881 CrossRef Medline
37. Schlaepfer, D. D., Hauck, C. R., and Sieg, D. J. (1999) Signaling through focal adhesion kinase. *Prog. Biophys. Mol. Biol.* **71,** 435–478 CrossRef Medline
38. Schlaepfer, D. D., and Hunter, T. (1996) Evidence for *in vivo* phosphorylation of the Grb2 SH2-domain binding site on focal adhesion kinase by Src-family protein-tyrosine kinases. *Mol. Cell Biol.* **16,** 5623–5633 CrossRef Medline
39. Miyamoto, S., Teramoto, H., Coso, O. A., Gutkind, J. S., Burbelo, P. D., Akiyama, S. K., and Yamada, K. M. (1995) Integrin function: Molecular hierarchies of cytoskeletal and signaling molecules. *J. Cell Biol.* **131,** 791–805 CrossRef Medline
40. Manders, E. M. M., Verbeek, F. J., and Ate, J. A. (1993) Measurement of co-localisation of objects in dual-colour confocal images. *J. Microsc.* **169,** 375–382 CrossRef Medline
41. Lambert, H., and Barragan, A. (2010) Modelling parasite dissemination: Host cell subversion and immune evasion by *Toxoplasma gondii*. *Cell Microbiol.* **12,** 292–300 CrossRef Medline
42. Margadant, C., Kreft, M., de Groot, D.-J., Norman, J. C., and Sonnenberg, A. (2012) Distinct roles of talin and kindlin in regulating integrin α5β1 function and trafficking. *Curr. Biol.* **22,** 1554–1563 CrossRef Medline
43. Lietha, D., Cai, X., Ceccarelli, D. F. J., Li, Y., Schaller, M. D., and Eck, M. J. (2007) Structural basis for the autoinhibition of focal adhesion kinase. *Cell* **129,** 1177–1187 CrossRef Medline
44. Kanchanawong, P., Shtengel, G., Pasapera, A. M., Ramko, E. B., Davidson, M. W., Hess, H. F., and Waterman, C. M. (2010) Nanoscale architecture of integrin-based cell adhesions. *Nature* **468,** 580–584 CrossRef Medline
45. Liu, J., Wang, Y., Goh, W. I., Goh, H., Baird, M. A., Ruehland, S., Teo, S., Bate, N., Critchley, D. R., Davidson, M. W., and Kanchanawong, P. (2015) Talin determines the nanoscale architecture of focal adhesions. *Proc. Natl. Acad. Sci. U.S.A.* **112,** E4864–E4873 CrossRef Medline
46. Webb, D. J., Donais, K., Whitmore, L. A., Thomas, S. M., Turner, C. E., Parsons, J. T., and Horwitz, A. F. (2004) FAK–Src signalling through paxillin, ERK and MLCK regulates adhesion disassembly. *Nat. Cell Biol.* **6,** 154–161 CrossRef Medline
47. Yano, H., Mazaki, Y., Kurokawa, K., Hanks, S. K., Matsuda, M., and Sabe, H. (2004) Roles played by a subset of integrin signaling molecules in cadherin-based cell-cell adhesion. *J. Cell Biol.* **166,** 283–295 CrossRef Medline
48. Lim, Y., Lim, S.-T., Tomar, A., Gardel, M., Bernard-Trifilo, J. A., Chen, X. L., Uryu, S. A., Canete-Soler, R., Zhai, J., Lin, H., Schlaepfer, W. W., Nalbant, P., Bokoch, G., Ilic, D., Waterman-Storer, C., and Schlaepfer, D. D. (2008) PyK2 and FAK connections to p190Rho guanine nucleotide exchange factor regulate RhoA activity, focal adhesion formation, and cell motility. *J. Cell Biol.* **180,** 187–203 CrossRef Medline
49. Weis, S. M., Lim, S.-T., Lutu-Fuga, K. M., Barnes, L. A., Chen, X. L., Göthert, J. R., Shen, T.-L., Guan, J.-L., Schlaepfer, D. D., and Cheresh, D. A. (2008) Compensatory role for Pyk2 during angiogenesis in adult mice lacking endothelial cell FAK. *J. Cell Biol.* **181,** 43–50 CrossRef Medline
50. Fan, H., and Guan, J.-L. (2011) Compensatory function of Pyk2 protein in the promotion of focal adhesion kinase (FAK)-null mammary cancer stem cell tumorigenicity and metastatic activity. *J. Biol. Chem.* **286,** 18573–18582 CrossRef Medline
51. Ye, F., Petrich, B. G., Anekal, P., Lefort, C. T., Kasirer-Friede, A., Shattil, S. J., Ruppert, R., Moser, M., Fässler, R., and Ginsberg, M. H. (2013) The mechanism of kindlin-mediated activation of integrin αIIbβ3. *Curr. Biol.* **23,** 2288–2295 CrossRef Medline
52. Fukuda, K., Bledzka, K., Yang, J., Perera, H. D., Plow, E. F., and Qin, J. (2014) Molecular basis of kindlin-2 binding to integrin-linked kinase pseu-

dokinase for regulating cell adhesion. *J. Biol. Chem.* **289,** 28363–28375 CrossRef Medline

53. Boothroyd, J. C., and Dubremetz, J.-F. (2008) Kiss and spit: The dual roles of *Toxoplasma* rhoptries. *Nat. Rev. Microbiol.* **6,** 79–88 CrossRef Medline
54. Weidner, J. M., Kanatani, S., Uchtenhagen, H., Varas-Godoy, M., Schulte, T., Engelberg, K., Gubbels, M. J., Sun, H. S., Harrison, R. E., Achour, A., and Barragan, A. (2016) Migratory activation of parasitized dendritic cells by the protozoan *Toxoplasma gondii* 14–3-3 protein. *Cell Microbiol.* **18,** 1537–1550 CrossRef Medline
55. Persat, F., Mercier, C., Ficheux, D., Colomb, E., Trouillet, S., Bendridi, N., Musset, K., Loeuillet, C., Cesbron-Delauw, M.-F., and Vincent, C. (2012) A synthetic peptide derived from the parasite *Toxoplasma gondii* triggers human dendritic cells' migration. *J. Leukoc. Biol.* **92,** 1241–1250 CrossRef Medline
56. Aliberti, J., Valenzuela, J. G., Carruthers, V. B., Hieny, S., Andersen, J., Charest, H., Reis e Sousa, C., Fairlamb, A., Ribeiro, J. M., and Sher, A. (2003) Molecular mimicry of a CCR5 binding-domain in the microbial activation of dendritic cells. *Nat. Immunol.* **4,** 485–490 CrossRef Medline
57. Morgado, P., Sudarshana, D. M., Gov, L., Harker, K. S., Lam, T., Casali, P., Boyle, J. P., and Lodoen, M. B. (2014) Type II *Toxoplasma gondii* induction of CD40 on infected macrophages enhances interleukin-12 responses. *Infect. Immun.* **82,** 4047–4055 CrossRef Medline
58. Horzum, U., Ozdil, B., and Pesen-Okvur, D. (2014) Step-by-step quantitative analysis of focal adhesions. *MethodsX* **1,** 56–59 CrossRef Medline
59. Livak, K. J., and Schmittgen, T. D. (2001) Analysis of relative gene expression data using real-time quantitative PCR and the $2^{-\Delta\Delta CT}$ method. *Methods* **25,** 402–408 CrossRef Medline
60. Wong, B. C. K., Chan, K. C. A., Chan, A. T. C., Leung, S. F., Chan, L. Y. S., Chow, K. C. K., and Lo, Y. M. D. (2006) Reduced plasma RNA integrity in nasopharyngeal carcinoma patients. *Clin. Cancer Res.* **12,** 2512–2516 CrossRef Medline